

Article (refereed) - postprint

Mekhalfi, Malika; Puppo, Carine; Avilan, Luisana; Lebrun, Regine; Mansuelle, Pascal; Maberly, Stephen C.; Gontero, Brigitte. 2014. **Glyceraldehyde-3-phosphate dehydrogenase is regulated by ferredoxin-NADP reductase in the diatom *Asterionella formosa***. *New Phytologist*, 203 (2). 414-423.
[10.1111/nph.12820](https://doi.org/10.1111/nph.12820)

© 2014 The Authors. *New Phytologist* © 2014 New Phytologist Trust

This version available <http://nora.nerc.ac.uk/507516/>

NERC has developed NORA to enable users to access research outputs wholly or partially funded by NERC. Copyright and other rights for material on this site are retained by the rights owners. Users should read the terms and conditions of use of this material at <http://nora.nerc.ac.uk/policies.html#access>

This document is the author's final manuscript version of the journal article, incorporating any revisions agreed during the peer review process. Some differences between this and the publisher's version remain. You are advised to consult the publisher's version if you wish to cite from this article.

The definitive version is available at <http://onlinelibrary.wiley.com/>

Contact CEH NORA team at
noraceh@ceh.ac.uk

**Glyceraldehyde-3-phosphate dehydrogenase is regulated by ferredoxin-NADP reductase
in the diatom *Asterionella formosa***

Malika Mekhalfi^a, Carine Puppo^a, Luisana Avilan^a, Régine Lebrun^c, Pascal Mansuelle^c
Stephen C. Maberly^d and Brigitte Gontero^a

^aAix-Marseille Université CNRS, BIP UMR 7281, 31 Chemin Joseph Aiguier, 13402
Marseille Cedex 20, France

^cPlate-forme Protéomique, FR3479, IBiSA Marseille-Protéomique IMM-CNRS, 31 Chemin
Joseph Aiguier, 13402 Marseille Cedex 20, France

^dCentre for Ecology & Hydrology, Lake Ecosystems Group, Lancaster Environment Centre,
Library Avenue, Bailrigg, Lancaster LA1 4AP UK

Running title: Regulatory properties of diatom GAPDH

Corresponding author: Dr B. Gontero

CNRS-BIP, 31 Chemin Joseph Aiguier, 13 402 Marseille Cedex 20 France

Email : bmeunier@imm.cnrs.fr

Phone : 33 4 91 16 45 49

Fax : 33 4 91 16 46 89

ABSTRACT

Diatoms are a widespread and ecologically important group of heterokont algae that contribute about 20% to global productivity. Previous work has shown that regulation of key Calvin cycle enzymes in diatoms differs from that of the Plantae, and that in crude extracts, glyceraldehyde-3-phosphate dehydrogenase (GAPDH) can be inhibited by NADPH under oxidizing conditions. Here, chromatography, mass spectrometry and sequence analysis showed that in the freshwater diatom, *Asterionella formosa*, GAPDH can interact with ferredoxin-NADP reductase (FNR) from the primary phase of photosynthesis, and the small chloroplast protein, CP12. In contrast, the ternary complex between GAPDH, phosphoribulokinase (PRK) and CP12, that is widespread in Plantae and cyanobacteria, was absent. Surface plasmon resonance measurements confirmed that GAPDH and FNR are able to interact. Activity measurements under oxidizing conditions, showed that NADPH can inhibit GAPDH-CP12 in the presence of FNR from *A. formosa* or *Spinacia oleracea*, explaining the earlier observed inhibition within crude extracts. Diatom plastids have distinctive attributes including the lack of the oxidative pentose phosphate pathway and so cannot produce NADPH in the dark. The observed down-regulation of GAPDH may allow NADPH to be re-routed towards other reductive processes contributing to their ecological success.

Keywords: CP12, FNR, GAPDH, protein-protein interaction

INTRODUCTION

Photosynthesis is the cornerstone of life on Earth and controls the atmospheric concentration of O₂ and CO₂ within global biogeochemical cycles. The diatoms (Heterokontophyta) are major players in this process, contributing about 20% to the global total (Armbrust, 2009). The evolutionary history of diatoms has resulted in a genome that differs from those of the better studied cyanobacteria, green algae and higher plants (Armbrust, 2009; Moustafa et al., 2009) giving rise to a characteristically different metabolism (Allen et al., 2011; Ast et al., 2009; Fabris et al., 2012; Kroth et al., 2008; Obata et al., 2013; Wilhelm et al., 2006).

Chloroplastic glyceraldehyde-3-phosphate dehydrogenase (GAPDH, EC 1.2.1.12), is a key enzyme within the Calvin cycle that catalyzes the reductive dephosphorylation of 1,3-bisphosphoglyceric acid (BPGA) to produce glyceraldehyde-3-phosphate (GAP) and inorganic phosphate, using NADH or preferentially NADPH (Trost et al., 2006). GAPDH has a strategic position within cell metabolism because GAP is an intermediate in many metabolic pathways, therefore GAPDH needs to be highly regulated. In cyanobacteria, green and red algae and higher plants, GAPDH and phosphoribulokinase (PRK, EC 2.7.1.19) are down-regulated by forming a ternary complex with CP12 (Carmo-Silva et al., 2011; Graciet et al., 2003; Howard et al., 2011; Marri et al., 2008; Oesterhelt et al., 2007; Wedel and Soll, 1998). CP12 is a small intrinsically disordered protein of about 8.5 kDa that is found in most photoautotrophs and cyanophages (Gontero and Maberly, 2012; Groben et al., 2010; Lopez-Calcano et al., 2014; Stanley et al., 2013; Thompson et al., 2011). The GAPDH-PRK-CP12 complex is well-characterized structurally and is responsible for inactivating the Calvin cycle in the dark (Avilan et al., 2012b; Fermani et al., 2012; Matsumura et al., 2011).

Despite the intriguing evolutionary features of diatoms and their importance in global primary productivity, relatively little is known about how their key enzymes are regulated. GAPDH from a freshwater diatom, *Asterionella formosa*, is known to interact with CP12 and consequently is redox-regulated (Erales et al., 2008). However, unlike other groups of algae, GAPDH from many chromalveolates is inhibited by NADPH in crude extracts and PRK is not redox-regulated (Maberly et al., 2010; Michels et al., 2005). The aim of this work was thus to determine the mechanism underlying the regulation of GAPDH in a diatom using *A. formosa* as a model.

RESULTS

Differential regulation of GAPDH activity

GAPDH in crude extracts was (i) strongly inhibited by incubation with NADPH and, (ii) stimulated by incubation with the reducing agent, DTT, or with NADP (Figure 1A). The addition of DTT to the GAPDH assays rapidly produced maximal activities in all treatments (Figure 1B). In contrast, the activity of the GAPDH-CP12 complex, purified as in (Erales et al., 2008), was not affected by incubation with NADPH, but incubation with DTT and NADP still stimulated GAPDH activity (Figure 1C). Progress curves for these treatments showed that when DTT was added to the assay, the activity of the control and NADPH-treated sample was stimulated while the NADP-treated and DTT-treated samples were unaffected (Figure 1D).

The GAPDH-CP12 complex was then dissociated to produce GAPDH without CP12, (Figure 2). Two peaks were observed using size-exclusion chromatography. The protein in the first peak had a molecular mass of about 150 kDa and had NADPH-dependent GAPDH activity. This corresponded to the tetrameric form of GAPDH since using mass-spectrometry, the molecular mass of the monomer was 36.7 kDa (Mekhalfi et al., 2012) and is hereafter referred to as ‘GAPDH-alone’. This protein was homogeneous under SDS gel-electrophoresis and migrated with an apparent molecular mass of about 47 kDa as has been observed before ((Erales et al., 2008); Figure 2B). Quantitative Edman sequencing of this sample gave an estimated GAPDH purity of 86%, in agreement with the silver stained gel that showed only one major band. The protein in the second peak was recognised by antibodies raised against CP12 from *C. reinhardtii* (see insert, Figure 2C). It was not possible to detect any band for this peak under SDS-PAGE, and so MALDI-ToF analysis was performed. The molecular masses determined by size-exclusion chromatography (Figure 2A, ~8.4 kDa) and MALDI-ToF (Figure 2C, m/z of 8578.062 for the singly-charged ion) are consistent with the known molecular mass of this protein. Although it is unusual for an intrinsically disordered protein to migrate according to its actual molecular mass on a size-exclusion gel, a similar result has been found for a well-characterized CP12 from *C. reinhardtii* that elutes at about 30 kDa when alone (Kaaki et al., 2013) but at 8.5 kDa immediately after dissociation from the GAPDH-CP12 complex (B. Gontero and C. Puppo, unpublished results). Incubation of GAPDH-alone with NADPH, DTT or NADP had no effect on its activity and all progress curves were similar (Figure 1E,F).

The redox-regulation observed in the GAPDH-CP12 complex is consistent with an interaction with CP12. However, the cause of the inhibition of GAPDH by NADPH within the crude extracts was unclear and could involve interaction with proteins, or small molecules such as metabolites. To distinguish between these possibilities, small molecules were

removed from crude extracts by ammonium sulfate precipitation and size-exclusion chromatography. The inhibition by NADPH was still present in these samples: the activity in the crude extract of $446 \pm 33 \text{ nmol min}^{-1} \text{ mg}^{-1}$ was significantly ($P < 0.001$) inhibited, by 48%, on addition of NADPH, implicating protein-protein interactions as the cause of GAPDH inhibition. The increase in percent inhibition with increasing protein concentration in the crude extract also strongly suggested that protein-protein interactions are involved in the regulation of GAPDH activity (Figure 3).

A range of different proteins was assayed to test whether the inhibition of GAPDH by NADPH involves specific or non-specific protein interactions. The activity of the GAPDH-CP12 complex was not affected by addition of bovine serum albumin, ribulose-1,5-bisphosphate carboxylase-oxygenase (RubisCO, EC 4.1.1.39) or PRK (data not shown). We also tested the addition of ferredoxin-NADP⁺ reductase (FNR, EC 1.18.1.1) on GAPDH because FNR is inhibited by NADPH (Zanetti and Forti, 1966) and co-immunolocalized with GAPDH in pea (Negi et al., 2008). The addition of commercial FNR from *Spinacea oleracea* inhibited GAPDH activity by 40% under oxidizing conditions when NADPH was present (data not shown), and the effect was abolished by addition of DTT in agreement with the patterns observed in Figure 1. This inhibition is consistent with a possible interaction between these proteins and to check this, the affinity between spinach FNR and GAPDH-CP12 was measured using surface plasmon resonance. There was a strong interaction between GAPDH-CP12 and FNR with a very low dissociation constant (K_D ; Table 1). In the presence of NADPH, K_D was even lower and the association rate constant between FNR and GAPDH-CP12 (k_a) was about 4-fold greater. In the presence of NADP, or DTT, attempts to fit the curves gave standard errors that were higher than the parameters thereby indicating that binding was not occurring (Table 1).

Isolation and identification of a GAPDH-CP12-FNR- complex

Although the observed strong binding and inhibition of GAPDH from *A. formosa* by spinach FNR is circumstantial evidence for an interaction, the diatom FNR sequence is only about 45 to 49% similar to higher plant FNR (Table 2). Therefore, attempts were made to purify FNR to check if it also inhibited GAPDH. Furthermore, since GAPDH from *A. formosa* had a high affinity for spinach FNR in the presence of NADPH, attempts were also made to detect and characterize a GAPDH-CP12-FNR complex using this metabolite throughout the purification. Several lines of evidence are consistent with the presence of this complex. Firstly, in the presence of NADPH, GAPDH and FNR activities were detected in the same fractions

following anion-exchange chromatography (Figure 4A) and subsequent size-exclusion chromatography (Figure 4B), but in the presence of NADP they eluted in separate fractions (Figure 4C). The presence of FNR and GAPDH within the same fraction (Figure 4B) was confirmed unambiguously using an Orbitrap mass spectrometer following digestion with trypsin where the five top proteins were identified as either GAPDH or FNR using MASCOT search and a heterokont database. Secondly, the estimated molecular mass of the GAPDH-CP12-FNR fraction of about 299 ± 13 kDa (Figure B), based on size-exclusion chromatography is higher than the molecular masses of about 140 ± 15 kDa for GAPDH-CP12 (Figure 4C and (Erales et al., 2008)) and 110 ± 26 kDa for FNR observed when the GAPDH-CP12-FNR fraction was disrupted with NADP. Although we cannot rule out NADPH-induced self-oligomerization of GAPDH and/or FNR, surface plasmon resonance measurements show that these two enzymes are able to interact (Table 1), kinetic experiments show that FNR affects GAPDH activity in the presence of NADPH and size-exclusion chromatography shows that the two enzymes co-elute. Therefore these results provide multiple lines of evidence for the existence of a complex. Thirdly, CP12 must be present because the redox-regulation of GAPDH requires CP12 (Figure 1), and DTT was required to activate GAPDH (Figure 4). In contrast, while in most photosynthetic organisms, PRK co-purifies with GAPDH, here PRK activity was not detected in the disrupted GAPDH-CP12-FNR fractions, nor was the protein detected using Orbitrap mass spectrometry.

The FNR produced by disrupting the GAPDH-CP12-FNR complex was homogeneous under SDS-PAGE (Figure 4D) and Edman sequencing showed that FNR comprised 60% of the total protein fraction. The molecular mass of FNR on the SDS-PAGE was about 37 kDa. We confirmed that FNR from *A. formosa* also inhibits GAPDH and the extent of inhibition of GAPDH-CP12 by FNR from *A. formosa* was similar to that found with spinach FNR (Figure 5A). The inhibition was relieved by DTT addition (data not shown) as for *Spinacia* FNR. PRK and RubisCO had no effect on GAPDH and although GAPDH was inhibited by FNR, the presence of GAPDH did not inhibit FNR.

It is possible that superoxide-based regulation of NADPH could be the cause of the GAPDH inhibition since NADPH could reduce the flavin of FNR with electrons transferred to oxygen. However, experiments performed under anaerobic conditions, with FNR from *A. formosa*, produced similar results to those in the presence of oxygen (data not shown).

N-terminal sequences of *A. formosa* GAPDH and FNR

Edman sequencing degradation of the purified GAPDH and of the purified FNR, allowed the N-terminal sequences of the first 15 amino acid residues of GAPDH and FNR to be identified. The sequences of the mature proteins from *A. formosa* were aligned with published sequences derived from marine diatom genomes. There was a very high degree of homology between the N-terminal sequence for *A. formosa* and three published diatom sequences (Table 3), of 87% similarity for GAPDH and between 80 and 93% similarity for FNR. A possible CP12 sequence, AAKPAD, was found in the amino acids derived from N-terminal sequencing of the GAPDH-CP12 complex, but CP12 could not be unambiguously identified because of the high variability of the CP12 N-terminus (Groben et al., 2010). Quantitative Edman analysis of the GAPDH-CP12-FNR fraction gave a ratio of two moles of GAPDH to one mole of FNR. This could be consistent with a composition of 1 tetramer of GAPDH to 1 dimer of FNR to fit within the molecular mass obtained by size-exclusion chromatography while allowing for the presence of CP12.

DISCUSSION

Regulation of biochemical pathways is essential to match metabolic rates to the supply of resources, to prevent futile cycling and to ensure homeostasis (Giordano, 2013). It is being increasingly recognized that supra-molecular complexes are involved in the regulation of many metabolic pathways including glycolysis (Graham et al., 2007), the Krebs cycle (Sreere, 1987), the Calvin cycle (Gontero et al., 2006) and in the primary phase of photosynthesis (Joliot and Johnson, 2011). For instance, during cyclic electron transfer, FNR, that catalyzes the reversible electron transfer between ferredoxin and NADP(H) in the last step of the photosynthetic electron chain (Carrillo and Ceccarelli, 2003), can form a complex with cytochrome *b_f* in higher plant chloroplasts (Joliot and Johnson, 2011). In carbon assimilation, one of the most well-studied complexes involves the association between two Calvin cycle enzymes, GAPDH and PRK, along with the small chloroplast protein CP12 (Howard et al., 2008; Trost et al., 2006). This complex is widespread having been found in cyanobacteria, red algae, green algae and higher plants (Avilan et al., 2012b; Fermani et al., 2012; Matsumura et al., 2011; Oesterhelt et al., 2007). In diatoms, only the binary GAPDH-CP12 complex has been detected so far (Erales et al., 2008) and GAPDH is up-regulated when reduced and, as shown here, by NADP, as found in other photosynthetic organisms (Marri et al., 2005).

We report here that in the diatom, *A. formosa*, the GAPDH-CP12-PRK complex is absent and instead, GAPDH from the Calvin cycle forms a complex with CP12 and FNR from

the photochemical phase of photosynthesis. Edman degradation produced the N-terminal amino acid sequence of FNR and GAPDH and these align with those derived from genomic analysis. These sequences allow the start of the mature proteins to be identified for the first time. To confirm the *in vivo* interaction, additional methods such as yeast two-hybrid and fluorescence resonance energy transfer are needed, but these require the knowledge of genes sequences which at the moment are unavailable in *A. formosa*. Genome sequencing of this diatom is currently under investigation.

However, the existence of the GAPDH-CP12-FNR complex explains the previously observed inhibition of GAPDH by NADPH in diatoms, and other chromalveolates, a broad group including chrysophytes, cryptophytes, haptophytes and dinoflagellates, under oxidizing conditions (Avilan et al., 2012a; Boggetto et al., 2007; Maberly et al., 2010). This inhibition was also observed in the desmid *Staurastrum cingulum* (Maberly et al., 2010). In higher plants, immunological studies have shown that many Calvin cycle enzymes, including GAPDH and FNR, are associated with thylakoid membranes (Agarwal et al., 2009; Negi et al., 2008; Sainis et al., 2003; Suss et al., 1993). Furthermore, a docking model has shown that it is theoretically possible for GAPDH to form a complex with FNR in *Pisum sativum* (Negi et al., 2008). It is therefore possible that this complex is also present elsewhere but probably with different consequences for regulation.

The detailed physiological significance of the regulation of GAPDH by complex formation with FNR, rather than with PRK in Plantae and cyanobacteria, remains to be elucidated. However, it is likely to have implications for both carbon metabolism and light harvesting and photoprotection and possibly nitrogen metabolism. With regard to carbon metabolism for example, diatom chloroplasts lack both NADP-malate dehydrogenase (EC 1.1.1.82) that controls the malate valve (Backhausen et al., 1994; Ocheretina et al., 2000; Taniguchi and Miyake, 2012) and the oxidative pentose pathway that produces NADPH in the dark (Michels et al., 2005; Wilhelm et al., 2006). Therefore, the regulation of NADPH availability will be at a premium since it is required for e.g. fatty acid synthesis, isoprenoid synthesis, nitrite reduction and chlororespiration (Wilhelm et al., 2006). In addition, the inhibition of GAPDH by NADPH in the dark will avoid a futile cycle with glycolysis, a pathway present in diatom chloroplasts (Fabris et al., 2012; Kroth et al., 2008). Diatoms also lack NAD(P) dehydrogenase (NDH) and flavodiiron protein that are involved in auxiliary routes of electron flow using NADPH (Joliot and Johnson, 2011; Peltier et al., 2010). Moreover, in diatoms the de-epoxidation state of the diatoxanthin-diadinoxanthin cycle is

maintained in the dark and also requires NADPH (Cruz et al., 2011). Therefore, in the dark, switching off GAPDH, the major consumer of NADPH, may be crucial in diatoms.

Diatoms evolved relatively recently, perhaps as early as 250 Ma ago, but are one of the most successful groups of algae comprising over 200,000 species found in virtually all habitats on Earth and responsible for about 20% of total global productivity (Armbrust, 2009). They have a very different evolutionary history compared to other algal lineages, with genes originating from bacteria, red and green algae and animals (Armbrust et al., 2004; Bowler et al., 2008; Moustafa et al., 2009; Wilhelm et al., 2006). For example, in diatoms, like in other chromalveolates, the atypical chloroplastic GAPDH, GapC1 (Takishita et al., 2009), is believed to be derived from a NAD-specific, cytosolic enzyme (Liaud et al., 2000). The differential regulation of their Calvin cycle enzymes (Boggetto et al., 2007; Maberly et al., 2010; Michels et al., 2005), and in particular the new complex between GAPDH and FNR reported here, is likely to be one of the factors that affects their ecological niche and success.

METHODS

Culture Conditions

Asterionella formosa (CCAP 1005/19) was grown at 16.5°C, under agitation in Diatom Medium (Beakes et al., 1988), at about 50 $\mu\text{mol photon m}^{-2} \text{ s}^{-1}$ (400 to 700 nm) under a 14/10 hours light/dark regime.

Production of Crude Extract and Enzyme Purification

Cells were harvested at the end of the dark period by centrifugation at 3750 g for 15 min at 4°C. The crude extracts were prepared following (Erales et al., 2008) in buffers containing 0.1 mM of either NAD or NADPH.

To obtain the GAPDH-CP12 complex, the crude extract was purified using ionic exchange, size-exclusion and hydroxylapatite chromatography as described in (Erales et al., 2008). The GAPDH-CP12 complex was dissociated by incubation with 20 mM DTT and 15 μM BPGA for 20 min at 30°C and then 0.45 mg of protein was loaded again onto a Sephacryl S300 size-exclusion column (height = 42 cm, diameter = 1 cm) equilibrated with 30 mM Tris, 2 mM EDTA, 0.1 M NaCl, 2 mM cysteine, 0.1 mM NAD, pH 7.9. Two main peaks were observed, collected separately and concentrated. The peak corresponding to pure GAPDH was concentrated using Vivaspin (30 000 MWCO, PES, Sartorius) and the peak corresponding to CP12 was concentrated using Spin-X (5k MWCO, Corning). The size-exclusion column was calibrated with aldolase (150 kDa), bovine serum albumin (68 kDa) and cytochrome c (12.5 kDa) from bovine heart (Sigma). Absorbance at 280 nm was used to indicate the amount of protein in eluted fractions.

The GAPDH-CP12-FNR complex was purified using ion-exchange and size-exclusion chromatography (Sephacryl S300, height 90 cm, diameter 2.6 cm) including 0.1 mM NADPH in all steps. Purified FNR was produced from the GAPDH-CP12-FNR complex by dissociation with 20 mM DTT for 20 min at 30°C followed by separation on a Sephacryl S300 size-exclusion column (height 90 cm, diameter 2.6 cm) in the presence of 30 μM NADP. Fractions were collected separately and concentrated using Vivaspin (30 000 MWCO, PES, Sartorius). The size-exclusion column was calibrated with RubisCO (550 kDa), GAPDH (150 kDa); spinach PRK (80 kDa) and Peroxidase (50 kDa).

SDS-PAGE and Dot Blot Experiments

SDS-PAGE (12% acrylamide) was carried out in a Bio-Rad Mini Protean system. Proteins were stained with Coomassie Brilliant Blue R250 or silver nitrate. The second peak, obtained

after the disruption of the GAPDH-CP12 complex, was blotted onto a nitrocellulose membrane (0.45 μm , Schleicher and Schüll, Dassel, Germany) as described in (Erales et al., 2008) but using recombinant *Chlamydomonas reinhardtii* CP12 antibodies (1:5 000 dilution). The reliability of the antibodies was checked by reaction with CP12 from *C. reinhardtii*.

Activity Measurements and Kinetic Analysis

NADPH-dependent activity of GAPDH was measured as described in (Graciet et al., 2004). FNR activity was measured with 0.3 mM 2,6-Dichloroindophenol (DCIP; Sigma) and 0.15 mM NADPH, at 600 nm using an extinction coefficient of $20 \text{ mM}^{-1} \text{ cm}^{-1}$ to follow the decline in DCIP concentration. Protein concentrations were assayed with the Bio-Rad (Hercules, CA, USA) protein dye reagent, using bovine serum albumin as a standard (Bradford, 1976).

NADPH-GAPDH assays of crude extracts, co-purified GAPDH-CP12 and purified GAPDH, were incubated for 20 min on ice before measurement as follows: (i) without addition (untreated), (ii) with 20 mM DTT, (iii) with 1 mM NADP or (iv) with 1 mM NADPH. When GAPDH was inhibited by NADPH, reactivation was carried out by adding 10 mM reduced DTT to the same cuvette to distinguish between inhibition and inactivation. Experimental data were fitted to theoretical curves with Sigma Plot v 11.0 (Systat Software GmbH, Erkrath, Germany).

To test the effect of the addition of potential protein partners on the activity of the GAPDH-CP12 preparation, GAPDH-CP12 (6 μg) was incubated for 20 min at room temperature with 10 μg of: FNR from *Spinacia oleracea* (Sigma F0628), recombinant PRK from *Chlamydomonas reinhardtii* (Avilan et al., 1997), RubisCO from *A. formosa*, or BSA (Promega, Madison, USA) in the presence or absence of 1 mM NADPH. A control was carried out with GAPDH-CP12 alone in the same conditions. DTT was then added into the cuvettes at a final concentration of 10 mM. Identical tests were performed with *A. formosa* FNR (24 μg) purified as described above under aerobic and anaerobic conditions using nitrogen-bubbled solutions and an anaerobic glove box (Jacomex, Dagneux - France) with an oxygen concentration of less than 7 ppm.

Proteins were separated from other components to test whether the inhibition effect of NADPH within the crude extract was linked to the presence of small molecules. The crude extracts were incubated with ammonium sulfate (661 g L^{-1}) at 4°C for 20 min. The samples were centrifuged) at 4°C for 60 min at 13 528 g and the pellet was resuspended in extraction buffer and passed through a Sephadex® G-25 size-exclusion column (PD10, GE Healthcare

Life Sciences). The fractions corresponding to the void volume of the column (2.5 to 3.0 mL) were collected and later analyzed for GAPDH activity.

Surface Plasmon Resonance Measurement

Spinach FNR ($50 \mu\text{g mL}^{-1}$) was coupled through its amine groups to a carboxymethyl dextran-coated biosensor chip (CM5, Biacore, GE Healthcare) following the manufacturer's instructions. About 200 RU (resonance unit) were immobilized. The interaction with co-purified GAPDH-CP12 was studied at 23°C and $30 \mu\text{L min}^{-1}$ with a Biacore T100 using 10 mM HEPES , 50 mM NaCl , $\text{pH } 7.4$ as running buffer with (i) 0.2 mM NADPH ; (ii) 0.2 mM NADPH plus 5 mM DTT ; (iii) 0.2 mM NADP . The GAPDH-CP12 concentrations spanned from 10 to 800 nM . The analyte was injected for 3 min to record the association phase, then buffer was injected for 4 min to record the dissociation phase. Global fits of the exponential curves (sensorgrams) were produced using the Biacore T100 Evaluation software (v2.0), giving values for the dissociation (k_d) and association (k_a) rate constants with a 1:1 interaction model where one ligand molecule (here FNR) interacts with one analyte molecule (here GAPDH-CP12). The equilibrium-dissociating constant (K_D) is given by $K_D = k_d/k_a$.

Mass spectrometry analyses

The putative GAPDH-CP12-FNR complex from the size-exclusion chromatography was dialyzed (final solution 0.5 mM Tris , $1 \text{ mM ammonium bicarbonate}$, 0.1 mM NAD , $36 \mu\text{M EDTA}$, $0.6 \mu\text{M NaCl}$, $\text{pH } 7.9$) and reduced with 10 mM DTT in $50 \text{ mM ammonium bicarbonate}$, $\text{pH } 8.0$ for 1 h at 56°C , alkylated with $55 \text{ mM iodoacetamide}$ in $50 \text{ mM ammonium bicarbonate}$, $\text{pH } 8.0$, for 30 min at room temperature and digested with Trypsin (Sigma) for 3 h at 37°C . The trypsin reaction was stopped by adding $12.5\% \text{ TFA}$ in water (v/v) and the peptides were dried with a speed vacuum pump. Mass spectrometry was performed on a LTQ Velos Orbitrap mass spectrometer (Thermo Fisher) equipped with a nanospray ion source and coupled to a nano UPLC Ultimate 3000 (Dionex). Dried tryptic peptides were dissolved in $2\% \text{ acetonitrile}/0.05\% \text{ TFA}$ in water and desalted on a C18 nano trap (Acclaim PepMap100, $100 \mu\text{m} \times 2 \text{ cm}$, $5 \mu\text{m}$, 100 \AA , Dionex) mounted in a 6-port valve before elution onto a C18 column (Acclaim PepMap RSLC, $75 \mu\text{m} \times 150 \text{ mm}$, $2 \mu\text{m}$, 100 \AA , Dionex). Peptides were eluted with a linear gradient from 4 to 55% of mobile phase B ($20\% \text{ water}$, $80\% \text{ acetonitrile}/0.1\% \text{ formic acid}$) in A ($0.1\% \text{ formic acid}$ in water) for 30 min and then to 95% of mobile phase B for 5 min . The peptides were analyzed using a positive ion mode and one first scan event full MS in the Orbitrap, at $30\,000$ resolution, followed by one

scan event of a collision induced dissociation of the 10 top ion parents (MS/MS fragment analysis in the Orbitrap, at 7500 resolution and 150-1700 range).

Spectra were processed by Proteome Discoverer software (Thermo Fisher Scientific) and the identification protein search was performed by MASCOT (*in situ* license) using the following parameters: (i) merged databases from NCBI (641 426 sequences) including Bacillariophyta : (taxonomy ID: 2836) and *Escherichia coli* (taxonomy ID: 562); (ii) enzyme: trypsin; (iii) variable modifications: cysteine carbamidomethylation and methionine oxidation; (iv) mass values: monoisotopic; (v) protein mass: unrestricted peptide; (vi) mass tolerance: ± 10 ppm; (vii) fragment mass tolerance: ± 0.3 Da; (viii) missed cleavages: 2. Proteins were considered as identified when 2 unique peptides with ion significance threshold $p < 0.05$ (>36 individual MASCOT ion score) or 5 consecutive b and y ion fragments were found.

N-terminal sequence determination

N-terminal sequence determination was performed by stepwise Edman degradation using an automatic sequencer model Procise 494 (Applied Biosystems). The protein solution in 30 mM Tris, 0.5 mM EDTA, 0.1 M NaCl, 0.1 mM NADPH and 10% glycerol, pH 7.9, was diluted with 100 μ l of 0.1% TFA in water, then desalted on the ProSorbTM sample preparation cartridge (Applied Biosystems) by 3 successive washes of 0.1% TFA in water. The 0.2 mm polyvinylidene fluoride (PVDF) membrane from the cartridge was excised, dried and put on the ProBlott[®] cartridge in the sequencer. A pulse-liquid PVDF program was run on 21, forty-minute cycles and phenylthiohydantoin (PTH)-amino acids were identified by HPLC using a Brownlee C18 column (5 μ m, 220 x 2.1 mm) with an eighteen minute gradient of B (acetonitrile/isopropanol, v/v) in A (THF 3.5% in water / premix 2 % (v/v)) from 18 to 53 % B, at 55°C, wavelength set at 269 nm. A solution of nineteen PTH-amino acid Standard (10 pmol) was used for calibration. Edman sequencing allowed the molar ratio of GAPDH to FNR to be determined based on the quantity of stable PTH-amino acids specific to GAPDH (Ile, Leu) or FNR (Val) in the first 20 amino acid sequenced and using the PTH-amino acid Standard solution at 10 pmol (Applied Biosystems).

Phylogenetic analyses

Sequences of GAPDH and FNR obtained were aligned with published sequences from marine diatom genomes using default values in ClustalW2

(<http://www.ebi.ac.uk/Tools/msa/clustalw2/>). Percent similarity between published sequences of FNR from diatoms and *Spinacia oleracea* were compared using ClustalW2.

ACKNOWLEDGMENTS

This work was supported in part by the Agence Nationale de la Recherche ANR-09-CP2D-06-01 and ANR SPINFOLD n° 09-BLAN-0100, the Centre National de la Recherche Scientifique (CNRS) and Aix-Marseille Université. The authors are grateful to the Conseil Régional of PACA and the city of Marseille for financial support in the acquisition of instrumentation. SCM was supported by the Natural Environment Research Council and LA and SCM received Visiting Scholarships from the Université Aix-Marseille. We thank CRCM proteomics staff from MaP, Emilie Baudalet and Stéphane Audebert, for the Orbitrap analyses and Carole Baffert from BIP for help with the anaerobic experiments.

Figure legends

Figure 1. Effect of NADPH, NADP and DTT on the Activity of GAPDH in *A. formosa* at Different Levels of Purity.

(A, B) Crude extracts

(C, D) GAPDH/CP12 purified using DEAE-Trisacryl, size-exclusion and hydroxylapatite chromatography

(E, F) Purified GAPDH-alone.

Activities per unit protein (A, C, E) shown as the mean with standard deviation (n = 3 to 8) for untreated control samples and samples pre-incubated with 1 mM NADPH; 1 mM NADP; and 20 mM DTT. Statistical difference from the untreated control: NS, not significant; *, P<0.05; **, P<0.01; ***, P<0.001. Time-course of product (P) appearance for the untreated control (●) and for the samples treated with 1 mM NADPH (○); 1 mM NADP (□); and 20 mM DTT (▲). The vertical arrow shows the addition of 10 mM DTT (final concentration) to the cuvettes. The total amount of protein in the cuvettes was 9.8, 0.19 and 0.10 μg in B, D and F respectively.

Figure 2. Purification of GAPDH from *A. formosa*.

(A) Disruption and separation of the GAPDH-CP12 complex using Sephacryl S300 chromatography. The GAPDH-CP12 complex was incubated with BPGA and DTT prior to loading onto the column. Total proteins were measured at 280 nm (●) and NADPH dependent activity of GAPDH (▲) was measured at 340 nm. The numbered arrows correspond to the elution volume (V_e) of aldolase (150 kDa, 1), BSA (68 kDa, 2) and cytochrome *c* (12.5 kDa, 3).

(B) SDS-PAGE of the purified *A. formosa* GAPDH. Proteins were separated on a 12% polyacrylamide gel under denaturing conditions and stained with silver nitrate. Lane 1, molecular weight markers (Precision Plus ProteinTM dual color standards, Bio-Rad); lane 2, GAPDH (<1 μg) obtained after disruption of the GAPDH-CP12 complex and after size-exclusion chromatography.

(C) Identification of CP12 by MALDI-ToF analysis and dot blot. The fractions corresponding to the second peak eluted from the Sephacryl S300 column, were pooled, concentrated and analyzed by MALDI-ToF and dot blot (see insert) using antibodies from *C. reinhardtii* CP12. The two spots correspond to CP12 from *C. reinhardtii* (1) and CP12 from *A. formosa* (2). The

m/z ratios observed at 4292.707 and 8578.062 correspond respectively to the doubly-charged ($z=2$) and singly-charged ($z=1$) ion of CP12.

Figure 3. Effect of Protein Concentration on the Inhibition of GAPDH Activity by NADPH. The curve of best-fit to a hyperbolic equation is shown.

Figure 4. Detection of the GAPDH-CP12-FNR Complex from *A. formosa* and Purification of FNR.

(A) Co-elution of GAPDH and FNR activity using anion-exchange chromatography. Data show absorbance at 280 nm (Δ), GAPDH activity measured under reduced conditions (\bullet), the FNR activity (\circ) and the NaCl gradient used to elute the protein on the anion-exchange column (- - -). No GAPDH activity could be detected under oxidizing conditions.

(B) Co-elution of GAPDH and FNR activity using size-exclusion chromatography. Proteins used as molecular weight standards were: 1. RubisCO (550 kDa), 2. GAPDH (150 kDa), 3. PRK (80 kDa) and 4. Peroxidase (50 kDa).

(C) Disruption and separation of the GAPDH-CP12-FNR complex. The GAPDH-CP12-FNR fraction was incubated with DTT prior to loading onto the Sephacryl S300 column in the presence of 30 μ M NADP.

(D) SDS-PAGE of the purified *A. formosa* FNR. Proteins were separated on 12% polyacrylamide gel under denaturing conditions and stained with Coomassie Blue. Lane 1, molecular weight markers (Euromedex, Unstained protein Ladder); lane 2, FNR (2 μ g) obtained after disruption of the GAPDH-CP12-FNR complex and after size-exclusion chromatography.

Figure 5. Effect on the Activity of *A. formosa* GAPDH-CP12 (G-C) of FNR and PRK from *A. formosa*, and RubisCO from *Chlamydomonas reinhardtii*.

Statistical difference from the untreated control: NS, not significant; ***, $P < 0.001$.

Table 1. Estimated Values of Association Rate Constant (k_a), Dissociation Rate Constant (k_d) and the Dissociation Constant (K_D) of the Interaction between FNR and GAPDH-CP12 Measured using Surface Plasmon Resonance. The running buffer was 10 mM HEPES, 50 mM NaCl, pH 7.4. Mean values are shown with standard deviation in parenthesis. No binding is indicated by ‘-’.

Addition to running buffer	k_a ($\text{mol}^{-1} \text{L s}^{-1}$)	k_d (s^{-1})	K_D (nmol L^{-1})
None	4.50 E+05 (0.72 E+05)	10.1 E-03 (1.26 E-03)	22.5 (4.5)
0.2 mM NADPH	1.73 E+06 (0.13 E+06)	12.4 E-03 (0.69 E-03)	7.2 (0.7)
0.2 mM NADPH plus 5 mM DTT	-	-	-
0.2 mM NADP	-	-	-

Table 2. Similarity score between mature proteins of FNR (identified using the N-terminal sequences in Table 3) for *Spinacia* and for three sequenced diatoms.

	<i>Spinacia oleracea</i>	<i>Thalassiosira pseudonana</i>	<i>Phaeodactylum tricornutum</i>	<i>Pseudo-nitzschia multiseries</i>
<i>Spinacia oleracea</i>	100	49	45	48
<i>Thalassiosira pseudonana</i>		100	84	87
<i>Phaeodactylum tricornutum</i>			100	85

Table 3. N-terminal Sequences of GAPDH and FNR from *A. formosa* Determined by Edman Degradation (in bold), Aligned with Published Sequences from other Diatoms using ClustalW2.

GAPDH	1	2	3	4	5	6	7	8	9	10	11	12	13	14	15
<i>Asterionella formosa</i>	S	T	G	M	G	I	N	G	F	G	R	I	G	R	L
<i>Thalassiosira pseudonana</i>	A	T	G	M	G	V	N	G	F	G	R	I	G	R	L
<i>Phaeodactylum tricornutum</i>	A	T	G	M	G	V	N	G	F	G	R	I	G	R	L
<i>Pseudo-nitzschia multiseriis</i>	A	T	G	M	G	V	N	G	F	G	R	I	G	R	L
Consensus symbols	:	*	*	*	*	:	*	*	*	*	*	*	*	*	*

FNR															
<i>Asterionella formosa</i>	(A)	Q	D	F	L	E	A	E	P	Y	Y	D	Q	S	T
<i>Thalassiosira pseudonana</i>	K	Q	D	F	L	E	A	E	P	Y	Y	S	Q	D	T
<i>Phaeodactylum tricornutum</i>	K	Q	N	F	L	E	A	E	P	Y	F	D	Q	S	T
<i>Pseudo-nitzschia multiseriis</i>		E	D	F	L	E	A	E	P	Y	Y	D	Q	S	T
Consensus symbols	:	:	*	*	*	*	*	*	*	*	:	.	*	.	*

Accession numbers for FNR are: *T. pseudonana*, gi|22401339|ref|XP_002295321.1; *P. tricornutum*, jgi|Phatr2|23717|estExt_gwp_gw1.C_chr_260086; *P.-N. multiseriis*, jgi|Psemu1|55817|gm1.55817_g. Accession numbers for GAPDH are: *T. pseudonana*, jgi|Thaps3|255092|thaps1_ua_pm.chr_1000239; *P. tricornutum*, jgi|Phatr2|22122|estExt_gwp_gw1.C_chr_150254; *P.-N. multiseriis*, jgi|Psemu1|35162|gm1.35162_g.

Consensus symbols are: (*) fully conserved residue; (:) conservation between residues with strong similar properties; (.) conservation between residues with weak similar properties. The residue in parenthesis was not unambiguously determined.

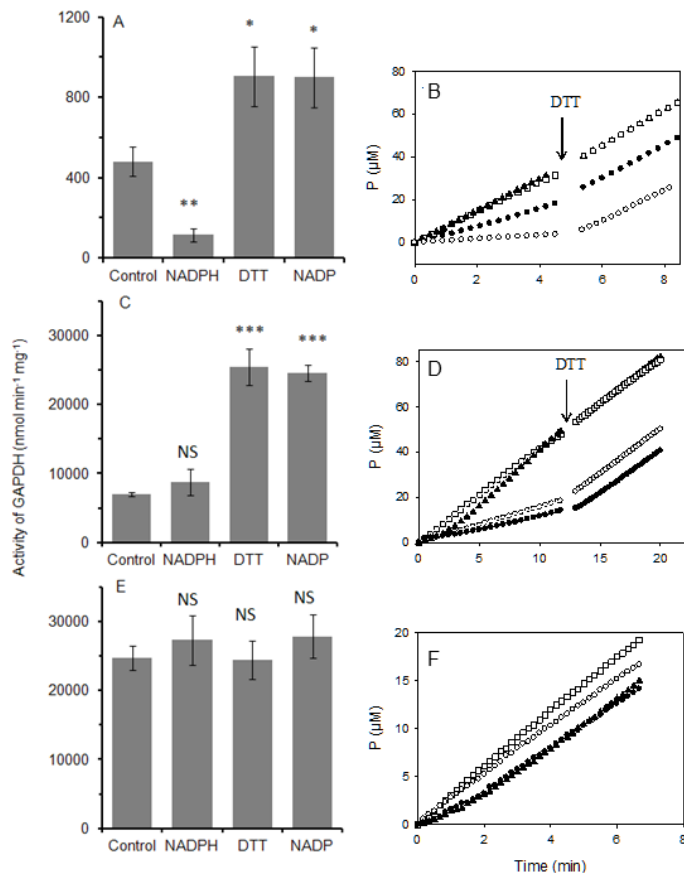


Figure 1. Effect of NADPH, NADP and DTT on the Activity of GAPDH in *A. formosa* at Different Levels of Purity.

(A, B) Crude extracts

(C, D) GAPDH/CP12 purified using DEAE-Trisacryl, size-exclusion and hydroxylapatite chromatography

(E, F) Purified GAPDH-alone.

Activities per unit protein (A, C, E) shown as the mean with standard deviation ($n = 3$ to 8) for untreated control samples and samples pre-incubated with 1 mM NADPH; 1 mM NADP; and 20 mM DTT. Statistical difference from the untreated control: NS, not significant; *, $P < 0.05$; **, $P < 0.01$; ***, $P < 0.001$. Time-course of product (P) appearance for the untreated control (\bullet) and for the samples treated with 1 mM NADPH (\circ); 1 mM NADP (\square); and 20 mM DTT (\blacktriangle). The vertical arrow shows the addition of 10 mM DTT (final concentration) to the cuvettes. The total amount of protein in the cuvettes was 9.8 , 0.19 and $0.10 \text{ }\mu\text{g}$ in B, D and F respectively.

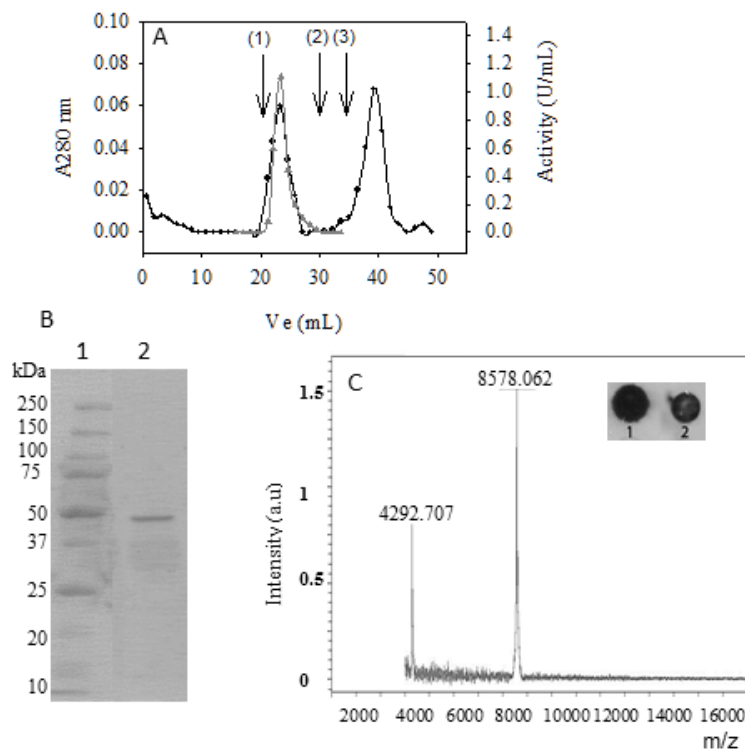


Figure 2. Purification of GAPDH from *A. formosa*.

(A) Disruption and separation of the GAPDH-CP12 complex using Sephacryl S300 chromatography. The GAPDH-CP12 complex was incubated with BPGA and DTT prior to loading onto the column. Total proteins were measured at 280 nm (●) and NADPH dependent activity of GAPDH (▲) was measured at 340 nm. The numbered arrows correspond to the elution volume (V_e) of aldolase (150 kDa, 1), BSA (68 kDa, 2) and cytochrome *c* (12.5 kDa, 3).

(B) SDS-PAGE of the purified *A. formosa* GAPDH. Proteins were separated on a 12% polyacrylamide gel under denaturing conditions and stained with silver nitrate. Lane 1, molecular weight markers (Precision Plus ProteinTM dual color standards, Bio-Rad); lane 2, GAPDH (<1 μ g) obtained after disruption of the GAPDH-CP12 complex and after size-exclusion chromatography.

(C) Identification of CP12 by MALDI-ToF analysis and dot blot. The fractions corresponding to the second peak eluted from the Sephacryl S300 column, were pooled, concentrated and analyzed by MALDI-ToF and dot blot (see insert) using antibodies from *C. reinhardtii* CP12. The two spots correspond to CP12 from *C. reinhardtii* (1) and CP12 from *A. formosa* (2). The m/z ratios observed at 4292.707 and 8578.062 correspond respectively to the doubly-charged ($z=2$) and singly-charged ($z=1$) ion of CP12.

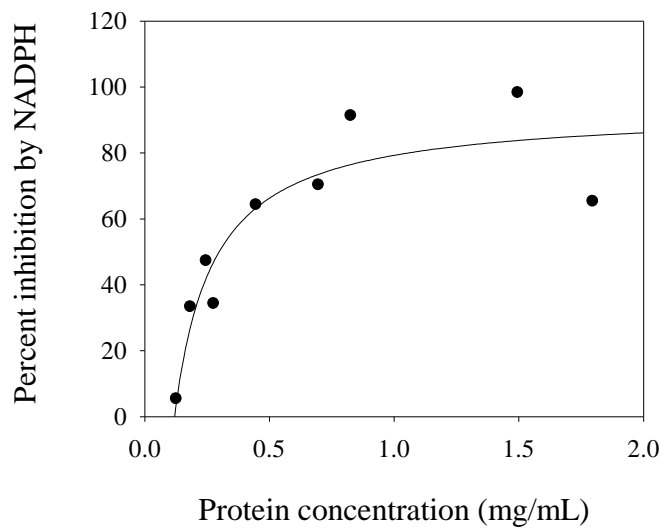


Figure 3. Effect of Protein Concentration on the Inhibition of GAPDH Activity by NADPH. The curve of best-fit to a hyperbolic equation is shown.

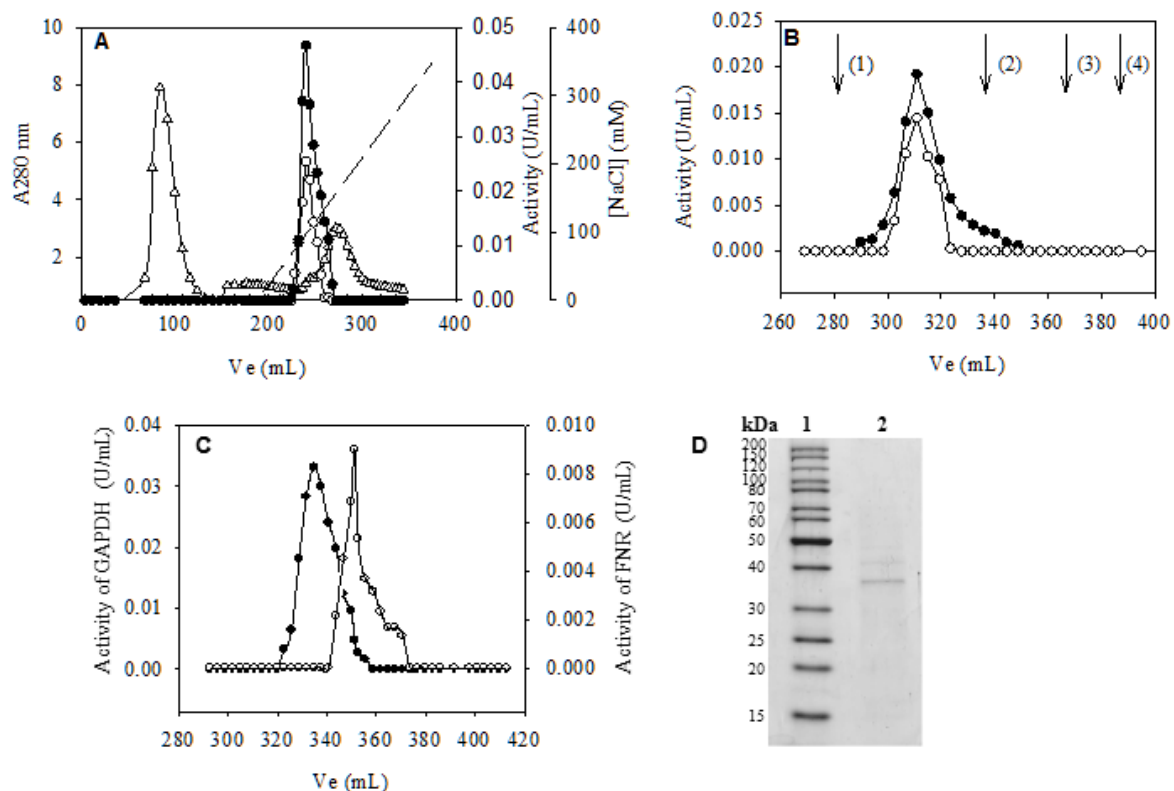


Figure 4. Detection of the GAPDH-CP12-FNR Complex from *A. formosa* and Purification of FNR.

(A) Co-elution of GAPDH and FNR activity using anion-exchange chromatography. Data show absorbance at 280 nm (Δ), GAPDH activity measured under reduced conditions (\bullet), the FNR activity (\circ) and the NaCl gradient used to elute the protein on the anion-exchange column (---). No GAPDH activity could be detected under oxidizing conditions.

(B) Co-elution of GAPDH and FNR activity using size-exclusion chromatography. Proteins used as molecular weight standards were: 1. RubisCO (550 kDa), 2. GAPDH (150 kDa), 3. PRK (80 kDa) and 4. Peroxidase (50 kDa).

(C) Disruption and separation of the GAPDH-CP12-FNR complex. The GAPDH-CP12-FNR fraction was incubated with DTT prior to loading onto the Sephacryl S300 column in the presence of 30 μ M NADP.

(D) SDS-PAGE of the purified *A. formosa* FNR. Proteins were separated on 12% polyacrylamide gel under denaturing conditions and stained with Coomassie Blue. Lane 1, molecular weight markers (Euromedex, Unstained protein Ladder); lane 2, FNR (2 μ g) obtained after disruption of the GAPDH-CP12-FNR complex and after size-exclusion chromatography.

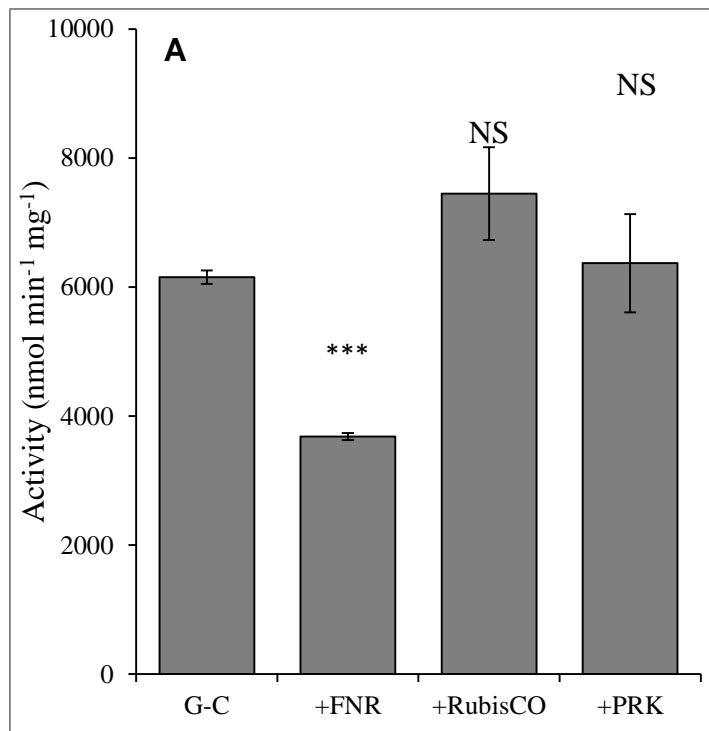


Figure 5. Effect on the Activity of *A. formosa* GAPDH-CP12 (G-C) of FNR and PRK from *A. formosa*, and RubisCO from *Chlamydomonas reinhardtii*.

Statistical difference from the untreated control: NS, not significant; ***, $P < 0.001$.

REFERENCES

- Agarwal, R., Ortleb, S., Sainis, J.K., and Melzer, M. (2009). Immunoelectron microscopy for locating Calvin cycle enzymes in the thylakoids of *Synechocystis* 6803. *Mol Plant* 2:32-42.
- Allen, A.E., Dupont, C.L., Obornik, M., Horak, A., Nunes-Nesi, A., McCrow, J.P., Zheng, H., Johnson, D.A., Hu, H., Fernie, A.R., et al. (2011). Evolution and metabolic significance of the urea cycle in photosynthetic diatoms. *Nature* 473:203-207.
- Armbrust, E.V. (2009). The life of diatoms in the world's oceans. *Nature* 459:185-192.
- Armbrust, E.V., Berges, J.A., Bowler, C., Green, B.R., Martinez, D., Putnam, N.H., Zhou, S., Allen, A.E., Apt, K.E., Bechner, M., et al. (2004). The genome of the diatom *Thalassiosira pseudonana*: ecology, evolution, and metabolism. *Science* 306:79-86.
- Ast, M., Gruber, A., Schmitz-Esser, S., Neuhaus, H.E., Kroth, P.G., Horn, M., and Haferkamp, I. (2009). Diatom plastids depend on nucleotide import from the cytosol. *Proc Natl Acad Sci U S A* 106:3621-3626.
- Avilan, L., Gontero, B., Lebreton, S., and Ricard, J. (1997). Information transfer in multienzyme complexes-2. The role of Arg64 of *Chlamydomonas reinhardtii* phosphoribulokinase in the information transfer between glyceraldehyde-3-phosphate dehydrogenase and phosphoribulokinase. *Eur J Biochem* 250:296-302.
- Avilan, L., Maberly, S.C., Mekhalfi, M., Plateau, J., Puppo, C., and Gontero, B. (2012a). Regulation of glyceraldehyde-3-phosphate dehydrogenase in the eustigmatophyte *Pseudocharaciopsis ovalis* is intermediate between a chlorophyte and a diatom. *European Journal of Phycology* 47:207-215.
- Avilan, L., Puppo, C., Eroles, J., Woudstra, M., Lebrun, R., and Gontero, B. (2012b). CP12 residues involved in the formation and regulation of the glyceraldehyde-3-phosphate dehydrogenase-CP12-phosphoribulokinase complex in *Chlamydomonas reinhardtii*. *Mol Biosyst* 8:2994-3002.
- Backhausen, J.E., Kitzmann, C., and Scheibe, R. (1994). Competition between electron acceptors in photosynthesis: Regulation of the malate valve during CO₂ fixation and nitrite reduction. *Photosynth Res* 42:75-86.
- Beakes, G., Canter, H.M., and Jaworski, G.H.M. (1988). Zoospores ultrastructure of *Zygorhizidium affluens* and *Z. planktonicum*, two chytrids parasitizing the diatom *Asterionella formosa*. *Can J Bot* 66:1054-1067.
- Boggetto, N., Gontero, B., and Maberly, S.C. (2007). Regulation of phosphoribulokinase and glyceraldehyde 3-phosphate dehydrogenase in a freshwater diatom, *Asterionella formosa* (Bacillariophyceae). *Journal of Phycology* 43:1227-1234.
- Bowler, C., Allen, A.E., Badger, J.H., Grimwood, J., Jabbari, K., Kuo, A., Maheswari, U., Martens, C., Maumus, F., O'tillar, R.P., et al. (2008). The *Phaeodactylum* genome reveals the evolutionary history of diatom genomes. *Nature* 456:239-244.
- Bradford, M.M. (1976). A rapid and sensitive method for the quantitation of microgram quantities of protein utilizing the principle of protein-dye binding. *Anal Biochem* 72:248-254.
- Carmo-Silva, A.E., Marri, L., Sparla, F., and Salvucci, M.E. (2011). Isolation and compositional analysis of a CP12-associated complex of calvin cycle enzymes from *Nicotiana tabacum*. *Protein Pept Lett* 18:618-624.
- Carrillo, N., and Ceccarelli, E.A. (2003). Open questions in ferredoxin-NADP⁺ reductase catalytic mechanism. *Eur J Biochem* 270:1900-1915.
- Cruz, S., Goss, R., Wilhelm, C., Leegood, R., Horton, P., and Jakob, T. (2011). Impact of chlororespiration on non-photochemical quenching of chlorophyll fluorescence and on the regulation of the diadinoxanthin cycle in the diatom *Thalassiosira pseudonana*. *J Exp Bot* 62:509-519.
- Eroles, J., Gontero, B., and Maberly, S.C. (2008). Specificity and function of glyceraldehyde-3-phosphate dehydrogenase in a freshwater diatom, *Asterionella formosa* (BACILLARIOPHYCEAE). *Journal of Phycology* 44:1455-1464.

- Fabris, M., Matthijs, M., Rombauts, S., Vyverman, W., Goossens, A., and Baart, G.J. (2012). The metabolic blueprint of *Phaeodactylum tricornutum* reveals a eukaryotic Entner-Doudoroff glycolytic pathway. *Plant J.* 70:1004-1014.
- Fermani, S., Trivelli, X., Sparla, F., Thumiger, A., Calvaresi, M., Marri, L., Falini, G., Zerbetto, F., and Trost, P. (2012). Conformational selection and folding-upon-binding of intrinsically disordered protein CP12 regulate photosynthetic enzymes assembly. *J Biol Chem* 287:21372-21383.
- Giordano, M. (2013). Homeostasis: an underestimated focal point of ecology and evolution. *Plant Sci* 211:92-101.
- Gontero, B., Avilan, L., and Lebreton, S. (2006). In: *Annual Plant Reviews--Plaxton, W.C., McManus, M.T., ed. Oxford: Blackwell Publishing* 187-218.
- Gontero, B., and Maberly, S.C. (2012). An intrinsically disordered protein, CP12: jack of all trades and master of the Calvin cycle. *Biochem Soc Trans* 40:995-999.
- Graciet, E., Gans, P., Wedel, N., Lebreton, S., Camadro, J.M., and Gontero, B. (2003). The small protein CP12: a protein linker for supramolecular assembly. *Biochemistry* 42:8163-8170.
- Graciet, E., Mulliert, G., Lebreton, S., and Gontero, B. (2004). Involvement of two positively charged residues of *Chlamydomonas reinhardtii* glyceraldehyde-3-phosphate dehydrogenase in the assembly process of a bi-enzyme complex involved in CO₂ assimilation. *Eur J Biochem* 271:4737-4744.
- Graham, J.W.A., Williams, T.C.R., Morgan, M., Fernie, A.R., Ratcliffe, R.G., and Sweetlove, L.J. (2007). Glycolytic enzymes associated dynamically with mitochondria in response to respiratory demand and support substrate channeling. *The Plant Cell Online* 19:3723-3738.
- Groben, R., Kaloudas, D., Raines, C.A., Offmann, B., Maberly, S.C., and Gontero, B. (2010). Comparative sequence analysis of CP12, a small protein involved in the formation of a Calvin cycle complex in photosynthetic organisms. *Photosynth Res* 103:183-194.
- Howard, T.P., Lloyd, J.C., and Raines, C.A. (2011). Inter-species variation in the oligomeric states of the higher plant Calvin cycle enzymes glyceraldehyde-3-phosphate dehydrogenase and phosphoribulokinase. *J Exp Bot* 62:3799-3805.
- Howard, T.P., Metodiev, M., Lloyd, J.C., and Raines, C.A. (2008). Thioredoxin-mediated reversible dissociation of a stromal multiprotein complex in response to changes in light availability. *Proc Natl Acad Sci U S A* 105:4056-4061.
- Joliot, P., and Johnson, G.N. (2011). Regulation of cyclic and linear electron flow in higher plants. *Proc Natl Acad Sci U S A* 108:13317-13322.
- Kaaki, W., Woudstra, M., Gontero, B., and Halgand, F. (2013). Exploration of CP12 conformational changes and of quaternary structural properties using electrospray ionization traveling wave ion mobility mass spectrometry. *Rapid Commun Mass Spectrom* 27:179-186.
- Kroth, P.G., Chiovitti, A., Gruber, A., Martin-Jezequel, V., Mock, T., Parker, M.S., Stanley, M.S., Kaplan, A., Caron, L., Weber, T., et al. (2008). A model for carbohydrate metabolism in the diatom *Phaeodactylum tricornutum* deduced from comparative whole genome analysis. *PLoS One* 3:e1426.
- Liaud, M.F., Lichtle, C., Apt, K., Martin, W., and Cerff, R. (2000). Compartment-specific isoforms of TPI and GAPDH are imported into diatom mitochondria as a fusion protein: evidence in favor of a mitochondrial origin of the eukaryotic glycolytic pathway. *Mol Biol Evol* 17:213-223.
- Lopez-Calcano, P.E., Howard, T.P., and Raines, C.A. (2014). The CP12 protein family: a thioredoxin-mediated metabolic switch? *Frontiers in Plant Science* 5:doi: 10.3389/fpls.2014.00009.
- Maberly, S.C., Courcelle, C., Groben, R., and Gontero, B. (2010). Phylogenetically-based variation in the regulation of the Calvin cycle enzymes, phosphoribulokinase and glyceraldehyde-3-phosphate dehydrogenase, in algae. *J Exp Bot* 61:735-745.
- Marri, L., Trost, P., Pupillo, P., and Sparla, F. (2005). Reconstitution and properties of the recombinant glyceraldehyde-3-phosphate dehydrogenase/CP12/phosphoribulokinase supramolecular complex of *Arabidopsis*. *Plant Physiology* 139:1433-1443.

- Marri, L., Trost, P., Trivelli, X., Gonnelli, L., Pupillo, P., and Sparla, F. (2008). Spontaneous assembly of photosynthetic supramolecular complexes as mediated by the intrinsically unstructured protein CP12. *J Biol Chem* 283:1831-1838.
- Matsumura, H., Kai, A., Maeda, T., Tamoi, M., Satoh, A., Tamura, H., Hirose, M., Ogawa, T., Kizu, N., Wadano, A., et al. (2011). Structure basis for the regulation of glyceraldehyde-3-phosphate dehydrogenase activity via the intrinsically disordered protein CP12. *Structure* 19:1846-1854.
- Mekhalfi, M., Avilan, L., Lebrun, R., Botbol, H., and Gontero, B. (2012). Consequences of the presence of 24-epibrassinolide, on cultures of a diatom, *Asterionella formosa*. *Biochimie* 94:1213-1220.
- Michels, A.K., Wedel, N., and Kroth, P.G. (2005). Diatom plastids possess a phosphoribulokinase with an altered regulation and no oxidative pentose phosphate pathway. *Plant Physiol* 137:911-920.
- Moustafa, A., Beszteri, B., Maier, U.G., Bowler, C., Valentin, K., and Bhattacharya, D. (2009). Genomic footprints of a cryptic plastid endosymbiosis in diatoms. *Science* 324:1724-1726.
- Negi, S.S., Carol, A.A., Pandya, S., Braun, W., and Anderson, L.E. (2008). Co-localization of glyceraldehyde-3-phosphate dehydrogenase with ferredoxin-NADP reductase in pea leaf chloroplasts. *J Struct Biol* 161:18-30.
- Obata, T., Fernie, A.R., and Nunes-Nesi, A. (2013). The central carbon and energy metabolism of marine diatoms. *Metabolites* 3:325-346.
- Ocheretina, O., Haferkamp, I., Tellioglu, H., and Scheibe, R. (2000). Light-modulated NADP-malate dehydrogenases from mossfern and green algae: insights into evolution of the enzyme's regulation. *Gene* 258:147-154.
- Oesterhelt, C., Klocke, S., Holtgreffe, S., Linke, V., Weber, A.P., and Scheibe, R. (2007). Redox regulation of chloroplast enzymes in *Galdieria sulphuraria* in view of eukaryotic evolution. *Plant Cell Physiol* 48:1359-1373.
- Peltier, G., Tolleter, D., Billon, E., and Cournac, L. (2010). Auxiliary electron transport pathways in chloroplasts of microalgae. *Photosynth Res* 106:19-31.
- Sainis, J.K., Dani, D.N., and Dey, G.K. (2003). Involvement of thylakoid membranes in supramolecular organisation of Calvin cycle enzymes in *Anacystis nidulans*. *J Plant Physiol* 160:23-32.
- Srere, P.A. (1987). Complexes of sequential metabolic enzymes. *Annu Rev Biochem* 56:89-124.
- Stanley, D.N., Raines, C.A., and Kerfeld, C.A. (2013). Comparative analysis of 126 cyanobacterial genomes reveals evidence of functional diversity among homologs of the redox-regulated CP12 protein. *Plant Physiol.* 161:824-835.
- Suss, K.H., Arkona, C., Manteuffel, R., and Adler, K. (1993). Calvin cycle multienzyme complexes are bound to chloroplast thylakoid membranes of higher plants in situ. *Proc Natl Acad Sci U S A* 90:5514-5518.
- Takishita, K., Yamaguchi, H., Maruyama, T., and Inagaki, Y. (2009). A hypothesis for the evolution of nuclear-encoded, plastid-targeted glyceraldehyde-3-phosphate dehydrogenase genes in "chromalveolate" members. *PLoS One* 4:e4737.
- Taniguchi, M., and Miyake, H. (2012). Redox-shuttling between chloroplast and cytosol: integration of intra-chloroplast and extra-chloroplast metabolism. *Curr Opin Plant Biol* 15:252-260.
- Thompson, L.R., Zeng, Q., Kelly, L., Huang, K.H., Singer, A.U., Stubbe, J., and Chisholm, S.W. (2011). Phage auxiliary metabolic genes and the redirection of cyanobacterial host carbon metabolism. *Proc Natl Acad Sci U S A* 108:757-764.
- Trost, P., Fermani, S., Marri, L., Zaffagnini, M., Falini, G., Scagliarini, S., Pupillo, P., and Sparla, F. (2006). Thioredoxin-dependent regulation of photosynthetic glyceraldehyde-3-phosphate dehydrogenase: autonomous vs. CP12-dependent mechanisms. *Photosynth Res* 89:1-13.
- Wedel, N., and Soll, J. (1998). Evolutionary conserved light regulation of Calvin cycle activity by NADPH-mediated reversible phosphoribulokinase/CP12/ glyceraldehyde-3-phosphate dehydrogenase complex dissociation. *Proc Natl Acad Sci U S A* 95:9699-9704.

- Wilhelm, C., Buchel, C., Fisahn, J., Goss, R., Jakob, T., Laroche, J., Lavaud, J., Lohr, M., Riebesell, U., Stehfest, K., et al. (2006). The regulation of carbon and nutrient assimilation in diatoms is significantly different from green algae. *Protist* 157:91-124.
- Zanetti, G., and Forti, G. (1966). Studies on the triphosphopyridine nucleotide-cytochrome f reductase of chloroplasts. *J Biol Chem* 241:279-285.